Supplementary Figures

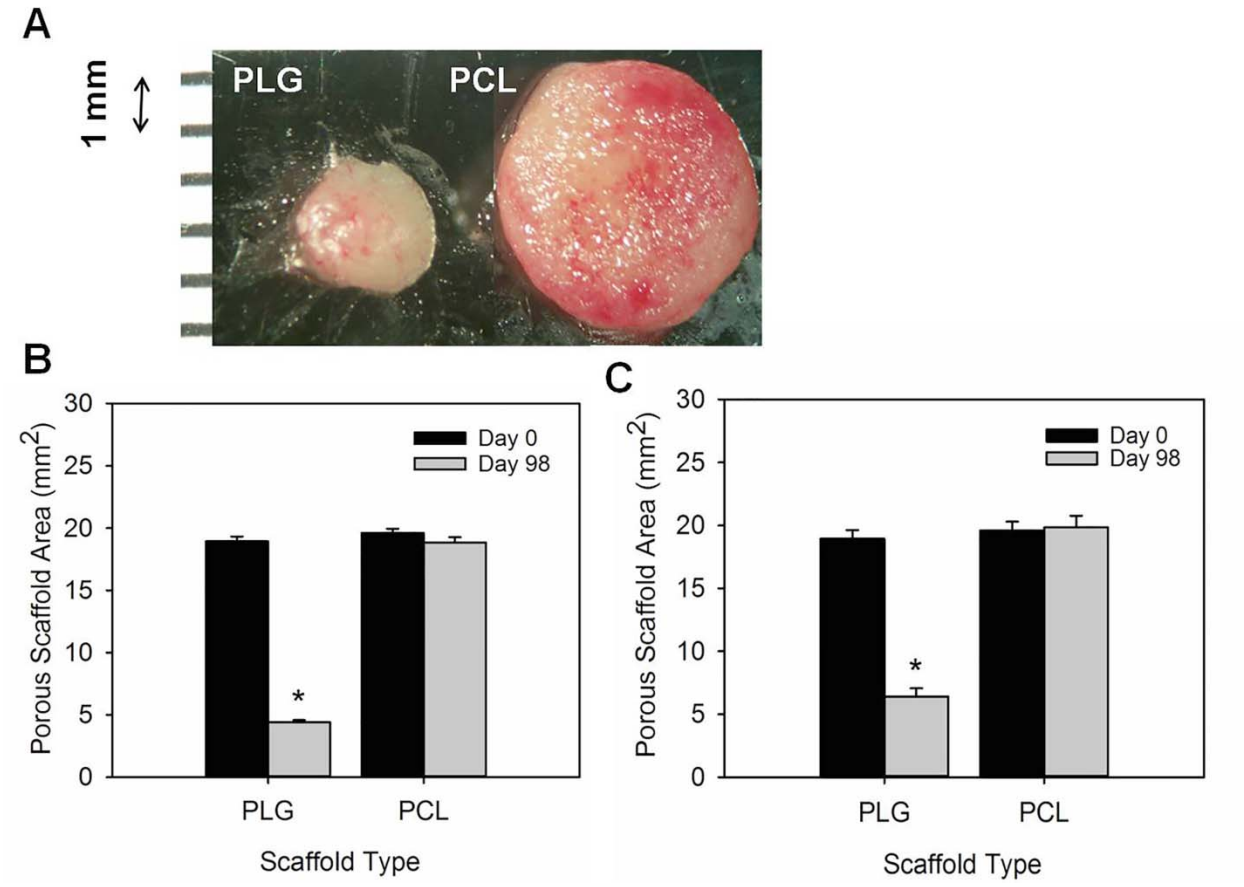

Figure S1: Micro-porous PCL scaffolds persist and maintain a space for extended times *in vivo.* (A) Representative photomicrographs of micro-porous PLG and PCL scaffolds retrieved from tumor free BALB/c mice at day 98 post scaffold implantation. Average scaffold area at day 0 versus day 98 for PLG and PCL scaffolds when tested in a BALB/c (B) and NSG (C) mouse model. N = 4; *$p < 0.0001$ compared to day 0 for PLG scaffolds in BALB/c and NSG mouse; $p = 0.22$ compared to day 0 for PCL scaffolds in BALB/c mouse and $p = 0.7$ compared to day 0 for PCL scaffolds in NSG mouse as determined by t-test. Scaffold area was calculated using dimensions obtained from images of scaffolds taken at day 0 and day 98 post implantation using Image J software (http://imagej.nih.gov/ij/). Error bars denote s.e.m.

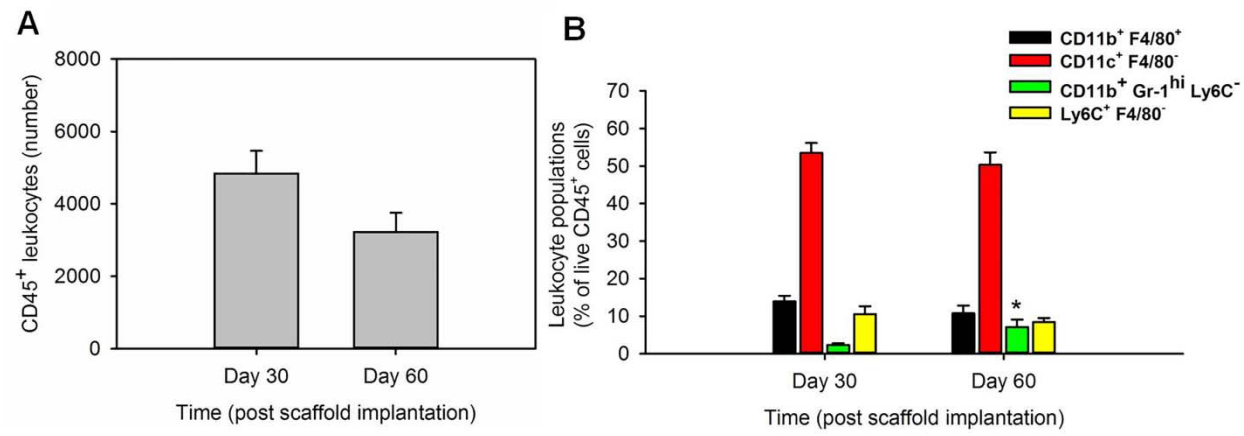

Figure S2: Host response following implantation of micro-porous PCL scaffolds in the dorsal subcutaneous space of an NSG mouse *in vivo*. (A) $CD45^+$ leukocyte numbers and (B) Dynamics of $CD11b^+F4/80^+$, $CD11c^+F4/80^-$, $CD11b^+Gr\text{-}1^{hi}Ly6C^-$, and $Ly6C^+F4/80^-$ populations expressed as a percentage of live $CD45^+$ leukocytes at day 30 and day 60 post PCL scaffold implantation ($N \geq 8$ for each time point examined, $^*p < 0.05$ compared to day 30 as determined by t-test). The relative distribution of immune cell populations was nearly identical between day 30 and day 60 post scaffold implantation. Error bars denote s.e.m.

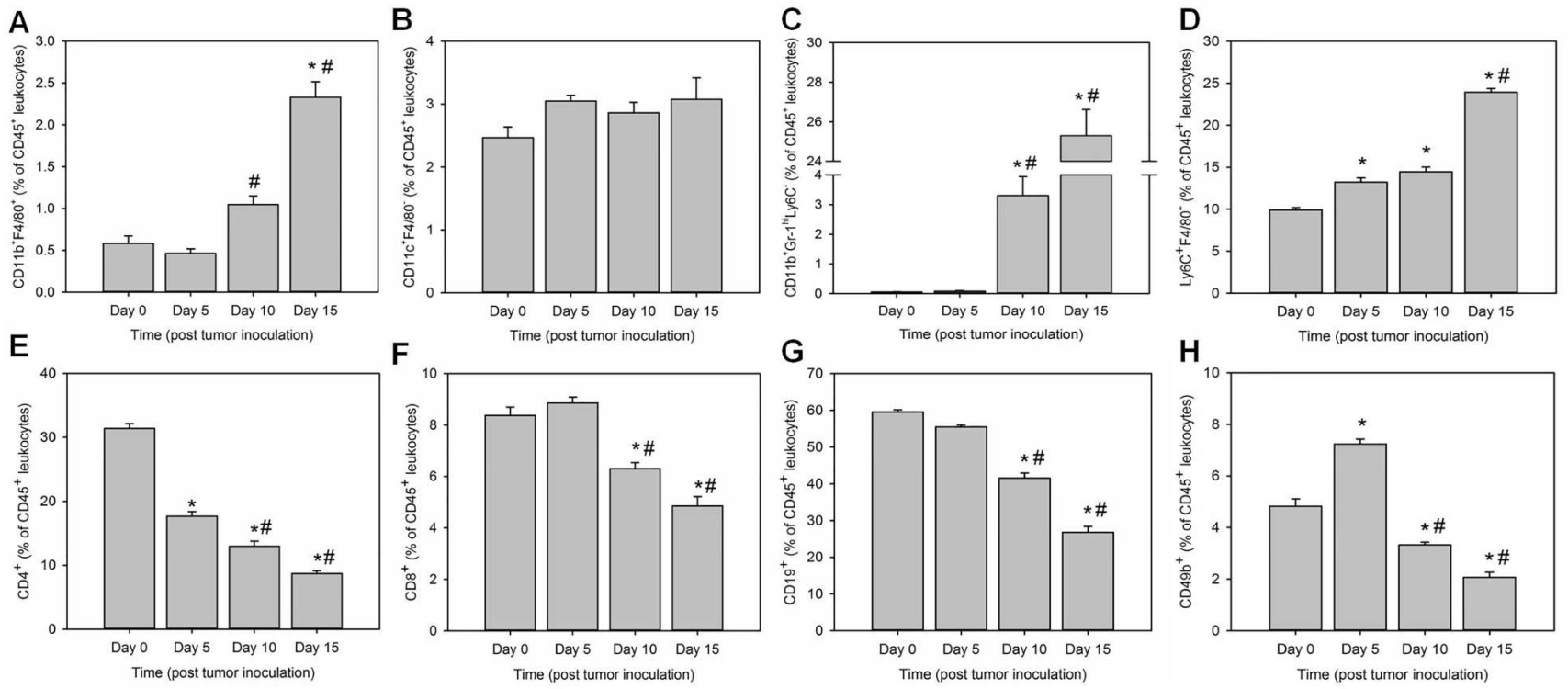

Figure S3: Dynamics of immune cell populations in the spleen of BALB/c mice with a PCL scaffold implant at day 0, 5, 10, and 15 post tumor inoculation. Percentage of (A) $CD11b^{+}F4/80^{+}$ (B) $CD11c^{+}F4/80^{-}$ (C) $CD11b^{+}Gr\text{-}1^{hi}Ly6C^{-}$ (D) $Ly6C^{+}F4/80^{-}$ innate immune cell populations and percentage of (E) $CD4^{+}$ (F) $CD8^{+}$ (G) $CD19^{+}$ and (H) $CD49b^{+}$ adaptive immune cell populations in the total population of live $CD45^{+}$ leukocytes. ($N \geq 5$ for each time point examined, *$p < 0.05$ compared to day 0 and #$p < 0.05$ compared to day 5 as determined by Tukey-HSD test post ANOVA). Error bars denote s.e.m.

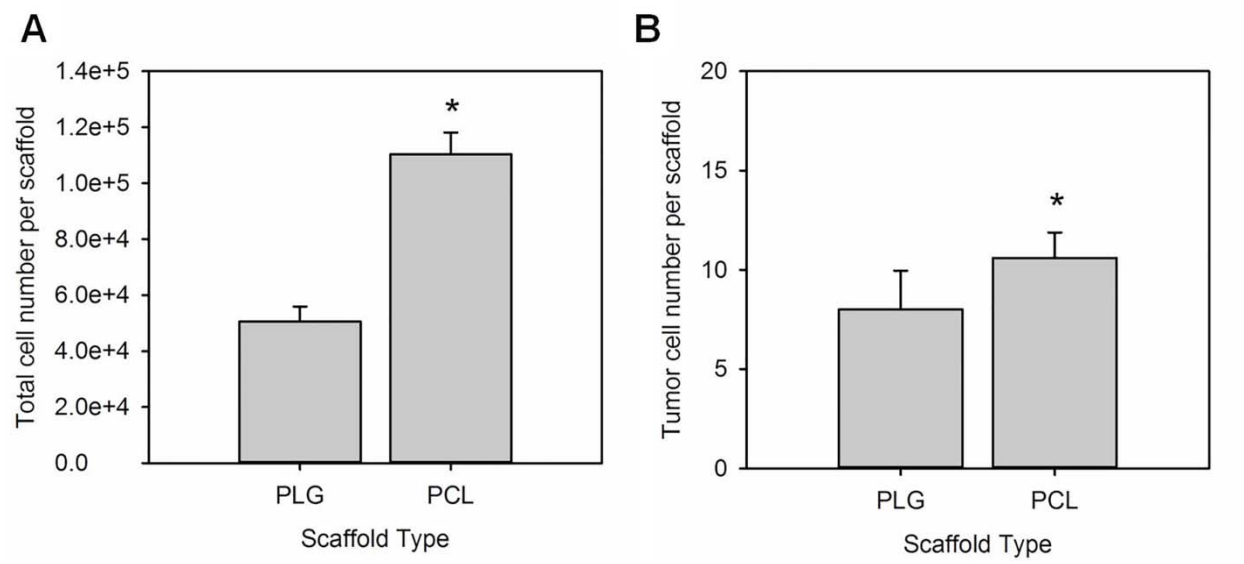

Figure S4: Micro-porous PCL scaffolds enable recruitment of human MDA-MD-231BR cells in a chronic model of scaffold implantation. (A) Total cell infiltration and (B) Tumor cell infiltration in PLG and PCL micro-porous scaffolds. Scaffolds were retrieved at day 15 post tumor inoculation, which was performed 1 month post scaffold implantation (N = 10 for each group, *$p < 0.05$ as determined by t-test for analysis of total cell numbers and Wilcoxon rank-sum test for tumor cell numbers). Error bars denote s.e.m.

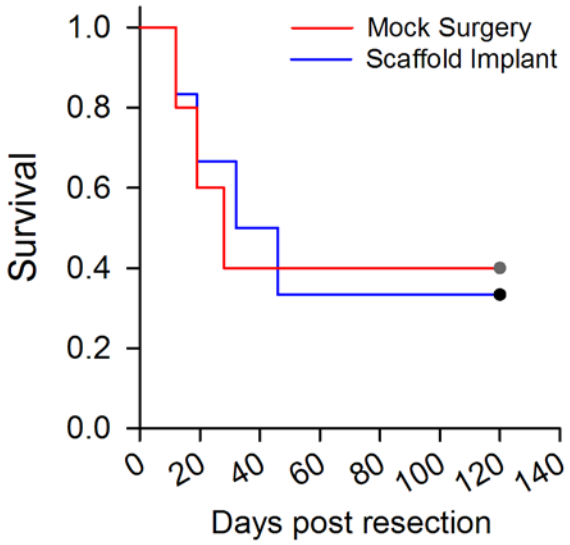

Figure S5: Micro-porous PCL scaffolds do not significantly improve survival in a post-surgical model of breast cancer metastasis with day 6 post tumor inoculation resection. ($N \geq 5$ for each group).

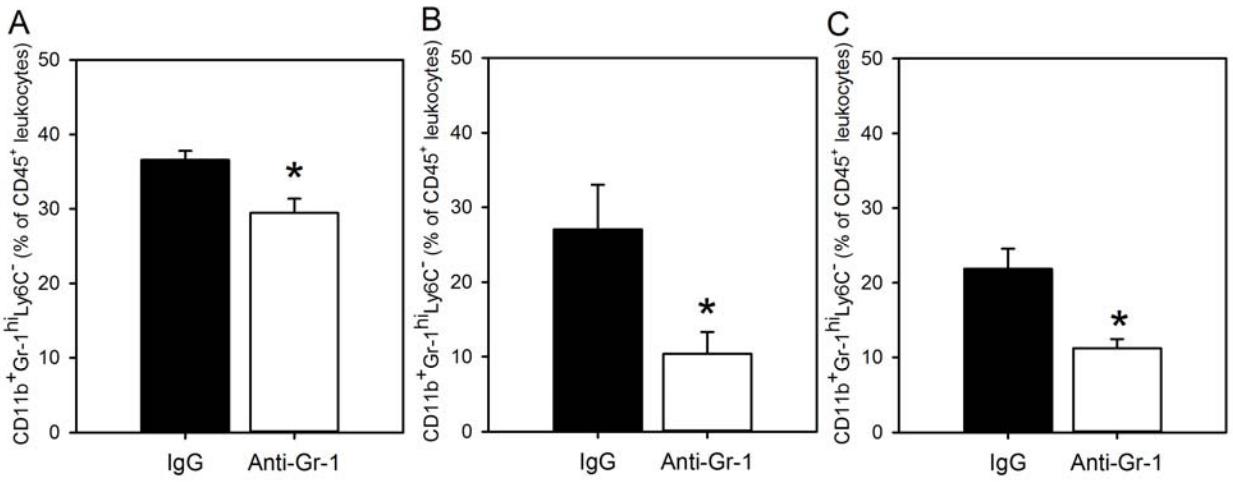

Figure S6: Anti-Gr-1 depletion significantly reduces the presence of $CD11b^{+}Gr\text{-}1^{hi}Ly6C^{-}$ MDSCs in the spleen (A) primary tumor (B) and scaffold (C). The percentage of $CD11b^{+}Gr\text{-}1^{hi}Ly6C^{-}$ cells in the $CD45^{+}$ leukocyte population was examined via flow cytometry at day 15 post tumor inoculation after three 300 μg antibody injections (day 5, 9, 13) (N=5 for spleen and primary tumor, N = 10 for scaffolds, performed in one experiment *$p<0.05$ as determined using t-test.) Error bars denote s.e.m.